Synthetic small molecule furin inhibitors derived from 2,5-dideoxystreptamine

Guan-Sheng Jiao*†, Lynne Cregar‡, Jinzhi Wang§, Sherri Z. Millis‡, Cho Tang*¶, Sean O'Malley*, Alan T. Johnson*, Sina Sareth*, Jason Larson§, and Gary Thomas§

Departments of *Chemistry and ‡Lead Discovery, PanThera Biopharma LLC, 99-193 Aiea Heights Drive, Suite 136, Aiea, HI 96701; and §Vollum Institute, Oregon Health and Science University, Portland, OR 97239

Edited by Donald F. Steiner, The University of Chicago, Chicago, IL, and approved November 7, 2006 (received for review July 31, 2006)

Furin plays a crucial role in embryogenesis and homeostasis and in diseases such as Alzheimer's disease, cancer, and viral and bacterial infections. Thus, inhibition of furin may provide a feasible and promising approach for therapeutic intervention of furin-mediated disease mechanisms. Here, we report on a class of small molecule furin inhibitors based on 2,5-dideoxystreptamine. Derivatization of 2,5-dideoxystreptamine by the addition of guanidinylated aryl groups yielded a set of furin inhibitors with nanomolar range potency against furin when assayed in a biochemical cleavage assay. Moreover, a subset of these furin inhibitors protected RAW 264.7 macrophage cells from toxicity caused by furin-dependent processing of anthrax protective antigen. These inhibitors were found to behave as competitive inhibitors of furin and to be relatively specific for furin. Molecular modeling revealed that these inhibitors may target the active site of furin as they showed site occupancy similar to the alkylating inhibitor decanoyl-Arg-Val-Lys-Arg-CH_2Cl. The compounds presented here are bona fide synthetic small molecule furin inhibitors that exhibit potency in the nanomolar range, suggesting that they may serve as valuable tools for studying furin action and potential therapeutics agents for furin-dependent diseases.

serine endoprotease | prohormone | proprotein convertase

Furin is a membrane-anchored, calcium-dependent serine endoprotease and is expressed in all tissues and cell lines examined (1–3). It is the first and, so far, the best-characterized member of the mammalian subtilisin-like family of prohormone/proprotein convertases (PCs), which convert precursors of many secreted proteins and peptide hormones into their biologically active forms (1–3). Furin is predominantly localized in the trans-Golgi network and cycles between this compartment, the cell surface, and the endosomes (2, 4). Hence, furin is able to access and efficiently process a diverse spectrum of substrates including growth factors, receptors, serum proteins, matrix metalloproteinases, viral envelope glycoproteins, and bacterial toxins, typically at sites with the consensus sequence Arg-Xaa-Lys/Arg-Arg$^{\downarrow}$ (2).

Although furin plays an essential role in embryogenesis and homeostasis, this endoprotease has also been implicated in the neurodegeneration associated with Alzheimer's disease, and tumor metastasis and the activation and virulence of many bacterial and viral pathogens (2). It has been demonstrated that furin inhibitors modulate tumor growth (5) and attenuate the toxicity of anthrax (6) and *Pseudomonas aeruginosa* (7) toxins and cytomegalovirus (8) in cell culture and animal models. Therefore, furin inhibitors hold great promise as potential therapeutic agents for treating furin-mediated diseases and viral and bacterial infections, particularly for short-term therapy.

To date, most furin inhibitors reported in the literature have been proteins (9–19) or peptides (20–24), which show excellent potency against furin, and largely mimic the substrate in binding the furin active site. The protein-based inhibitors include naturally occurring human proteinase inhibitor 8 (9), inter-α-inhibitor protein (10), and serpin Spn4A (11, 12) and bioengineered variants of α_1-antitrypsin [α_1-PDX (13) and analogs (14)], turkey ovomucoid third domain (15), α_2-macroglobulin mutants (16), and eglin c (17–19). The peptide-based inhibitors are represented by polyarginine peptides (20), peptidyl chloromethyl and aminomethyl ketones and ketomethylene pseudopeptides (21), isostere-containing cyclic peptides derived from barley serine proteinase inhibitor 2 (22), peptidyl boronic acids (17), peptides derived from the prosegment of furin (23), and α_1-PDX-derived peptides (24). The only reported nonprotein, nonpeptide inhibitors of furin are the natural products of the andrographolide family (25), their succinoyl ester derivatives (25), and certain metal complexes (26), all showing modest inhibitory activity against furin in the micromolar to millimolar range.

Our interest in furin inhibitors originated from a project aimed at developing efficient and innovative therapies for anthrax (27), an infectious disease of notoriety because of its potential use as a biowarfare and bioterrorism agent. Proteolytic cleavage of anthrax protective antigen (PA) (28) by furin (29) is an obligatory step for the entry of anthrax lethal factor (LF) (30) and edema factor (31) into the cytosol of host cells where they exert their toxic effects (32). Thus, inhibition of furin could offer an attractive therapeutic approach to combat anthrax intoxication (6). Herein, we report the discovery of synthetic small molecule furin inhibitors derived from 2,5-dideoxystreptamine that display nanomolar potency. The synthetic optimization of a lead compound identified from a focused screening is described, and the structure activity relationships are discussed. The enzyme specificity of these inhibitors for furin is also presented, and the possible binding mode of these inhibitors with furin through molecular modeling is presented. Finally, these inhibitors showed to protect cell killing by the furin-dependent processing and activation of anthrax PA.

Results

Identification of Furin-Inhibitory Lead Compound 1a. Our initial idea for furin inhibitors came from the finding that furin has a strong propensity for binding substrates and inhibitors containing positively charged groups such as arginine and lysine via electrostatic interaction (1–3, 33). Also, examination of the recently determined crystal structure of mouse furin (33) indicated that the active site of furin consists of a canyon-like groove that is lined with clusters of negatively charged residues, Asp-258 and Asp-306 (in the S1 subsite); Asp-154 and Asp-191 (S2); Glu-236 and Glu-264 (S4); Glu-257 (S5); and Glu-230 and Glu-233 (S6). Therefore, we hypothesized that small molecules having the proper spatial distribu-

Author contributions: G.-S.J., C.T., and G.T. designed research; G.-S.J., L.C., J.W., S.O., S.S., and J.L. performed research; G.-S.J., L.C., J.W., S.Z.M., A.T.J., J.L., and G.T. analyzed data; and G.-S.J., S.Z.M., S.O., A.T.J., and G.T. wrote the paper.

The authors declare no conflict of interest.

This article is a PNAS direct submission.

Abbreviations: PC, prohormone/proprotein convertase; PA, protective antigen; LF, lethal factor; FP, fusion protein; GADD, guanidinylated aryl 2,5-dideoxystreptamine derivative.

†To whom correspondence should be addressed. E-mail: gjiao@pantherabio.com.

¶Present address: Shanghai Hengrui Pharmaceuticals, Shanghai 200245, China.

This article contains supporting information online at www.pnas.org/cgi/content/full/0606555104/DC1.

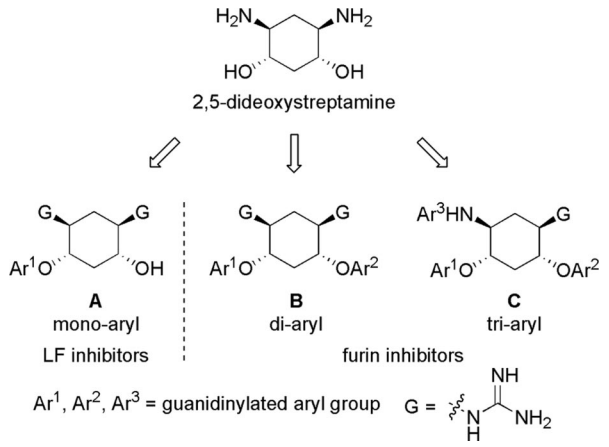

Fig. 1. 2,5-Dideoxystreptamine and its guanidinylated mono-aryl (*A*), di-aryl (*B*), and tri-aryl (*C*) substituted derivatives.

tion of positively charged groups might show inhibition against furin.

We set out to test the hypothesis by using our in-house collection of guanidinylated 2,5-dideoxystreptamine derivatives that had been shown to exhibit inhibition of anthrax LF (34). The *in vitro* biochemical assay results revealed that the set of guanidinylated mono-aryl substituted 2,5-dideoxystreptamine derivatives (Fig. 1*A*) tested show little or no inhibition against furin ($K_i > 100$ μM; data not shown). However, one guanidinylated di-aryl analog, compound **1a**, exhibited surprisingly high potency for furin ($K_i = 169$ nM; see Table 1), which suggested that the second aryl ring bearing positively charged guanidinyl groups provides the necessary interaction for binding to the active site of furin.

Synthesis of Guanidinylated Aryl 2,5-Dideoxystreptamine Derivatives (GADDs). To explore the above finding further, we prepared more di-aryl substituted compounds (Fig. 1*B*) analogous to compound **1a**. In addition, tri-aryl substituted compounds (Fig. 1*C*) were prepared to test their inhibition of furin. As outlined in Fig. 2*A*, the di-aryl substituted compounds **1b**–**1m** (see Table 1 for structures) were synthesized as described (34). In a similar manner, the tri-aryl substituted compounds **1n** and **1o** (Table 1) were prepared by the S_NAr coupling of three equivalents of nitro-substituted aryl halides with mono-Cbz-protected compound **7** as the key step (Fig. 2*B*). The di-carbamate compounds **1p**–**1r** (Table 1) were prepared by carbamation of **5** (Fig. 2*C*).

Inhibition of Furin by GADDs. The compounds synthesized were then assessed for their ability to inhibit furin *in vitro* by using a biochemical cleavage assay. The results of these experiments are given in Table 1 and allow for several interesting observations. First, compounds such as **1a**, **1b**, **1d**–**1g**, **1i**, and **1n** exhibited potent activities inhibiting furin in the nanomolar range. Second, although there was no linear correlation between the number of guanidinyl groups and inhibition of furin, four guanidinyl groups appear to give the best inhibitory activity (**1g** vs. **1a** and **1b**; **1e** vs. **1c**, and **1i** vs. **1m**). Third, the position of guanidinyl groups, particularly those on the aromatic ring, plays a critical role for furin inhibition. Substitution at *para*-position is superior to *ortho*-substitution (**1g** vs. **1h**, **1i** vs. **1j**, and **1p** vs. **1r**); analogs (**1h**, **1j**, and **1r**) that bear only an *ortho*-guanidinyl group showed very weak or no inhibitory activity against furin. Fourth, increasing the size of the R^1 group appears to result in a decrease in inhibitory activity (**1f** vs. **1g** and **1e**). It was also found that the di-aryl substituted compounds **1g** and **1f** showed better inhibitory activity than corresponding tri-aryl substituted analogs **1n** and **1o**. Finally, the linker between the aromatic fragment and 2,5-dideoxystreptamine also influences inhibitory potency, which is evident from the fact that replacement of the ether oxygen-atom with the carbamate group (-NHCOO-) resulted in a significant loss of inhibitory activity (**1p** vs. **1g**).

Mechanism of Furin Inhibition by GADDs. Mechanistic studies showed that the GADDs are competitive inhibitors of furin. For example, time- and concentration-dependent inactivation of furin by compound **1e** revealed that inhibition is competitive. Progress curves for the reaction of furin in the presence of several concentrations of compound **1e** and varying concentrations of substrate showed that initial velocity was inversely proportional to the concentration of inhibitor as shown by a Lineweaver–Burk reciprocal plot [supporting information (SI) Fig. 5*A*]. The K_i value deduced from this replot was 6 nM. A Dixon plot (SI Fig. 5*B*) generated from the same data set was also in agreement with a competitive mechanism of inhibition by this compound.

Furin Specificity of GADDs. To explore the specificity of the GADDs for furin, the most potent furin inhibitor compounds **1d**–**1g**, **1i**, and **1n** were counterscreened against several furin-related human PCs, such as PC6B, PC7, and PACE4, and a serin protease trypsin. Two metalloproteases, MT1-MMP and LF, were also tested for off-target activity. The K_i values from these experiments are summarized in Table 2. It was found that, although compounds **1d**–**1g**, **1i**, and **1n** showed comparable potency against furin and PC6B, these compounds preferentially inhibited furin over PACE4 by 2- to 10-fold and over PC7 by 11- to 76-fold. In addition, these compounds inhibited LF 25- to 167-fold less effectively than they did furin and showed no measurable inhibition against trypsin and MT1-MMP at the concentrations tested.

Molecular Modeling of GADDs Binding to Furin Active Site. To gain additional support for our initial hypothesis, we conducted *in silico* docking experiments that showed that the inhibitory GADDs are able to interact with negatively charged residues in the active site of furin. As illustrated in Fig. 3, *the docked pose of compound* **1n** shows similar occupancy of the major subsites S1, S2, and S4 when compared with the alkylating inhibitor decanoyl-Arg-Val-Lys-Arg-CH_2Cl, which was cocrystallized with truncated mouse furin (33). In particular, the *para*-guanidinophenyl R^2 group (see Table 1) penetrates deep into S1 occupying the same space as the P1 Arg$^{\downarrow}$. The di-aryl substituted GADDs such as compounds **1e** and **1g** show similar occupancy of the active site with the aryl groups occupying one or more of the three subsites S1, S2, and S4.

Cell-Based Inhibition of Furin by GADDs. The strongly inhibitory compounds **1a**, **1b**, **1d**–**1g**, **1i**, and **1n** identified in the *in vitro* biochemical assay (Table 1) were further evaluated for their efficacy toward inhibiting furin-dependent processing of anthrax PA in cultured RAW 264.7 macrophages. To avoid potential interference from the direct inhibition of anthrax LF (34), we chose to monitor PA processing by a well described fusion protein (FP) 59 (35), in which the catalytic domain of LF is replaced by that of *Pseudomonas* exotoxin A. This FP requires furin-processed PA for cellular entry and subsequent inhibition of protein synthesis and can be quantified by measuring the incorporation of ^{35}S[methionine] into a trichloroacetic acid-precipitated form (13). It was found that, whereas compounds **1d** and **1n** showed strong inhibition of PA processing with EC_{50} values of 4.2 and 12.9 μM, respectively, compound **1f** also inhibited PA processing to a lesser extent ($EC_{50} > 25$ μM) (Fig. 4). The rest of the compounds when tested showed no detectable inhibitory activity under the assay conditions (data not shown).

In a control experiment in the absence of furin and FP59 in the cell-based assay buffer solution, compounds **1a**, **1b**, **1d**–**1g**, **1i**, and **1n** showed no significant cytotoxicity to the cells at concentrations up to 250 μM (data not shown).

Table 1. Inhibition constants (K_i) for the 2,5-dideoxystreptamine-derived small molecules against furin

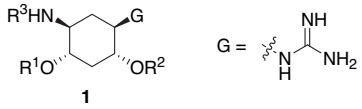

1

Compound	R^1	R^2	R^3	No. of guanidinyl groups	K_i, μM
1a	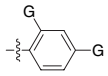	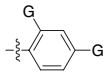		6	0.169 ± 0.009
1b	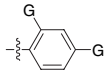	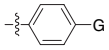		5	0.089 ± 0.022
1c	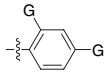	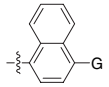		5	0.404 ± 0.018
1d	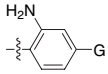	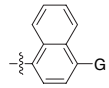		4	0.022 ± 0.002
1e	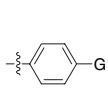	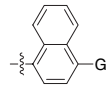		4	0.006 ± 0.002
1f	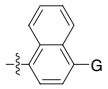	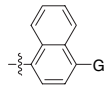		4	0.069 ± 0.004
1g	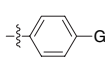	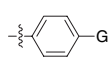		4	0.012 ± 0.003
1h	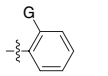	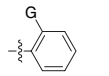		4	>100
1i	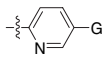	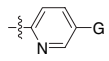		4	0.042 ± 0.003
1j	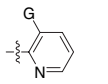	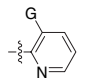		4	>100
1k	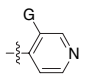	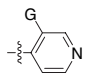		4	>100
1l	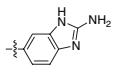	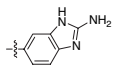		2	>100
1m	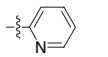	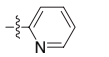		2	>100
1n				4	0.046 ± 0.003
1o				4	0.423 ± 0.005
1p				4	0.812 ± 0.041
1q				4	1.768 ± 0.007
1r				4	>100

The K_i values are expressed as the mean of three independent experiments ± SEM.

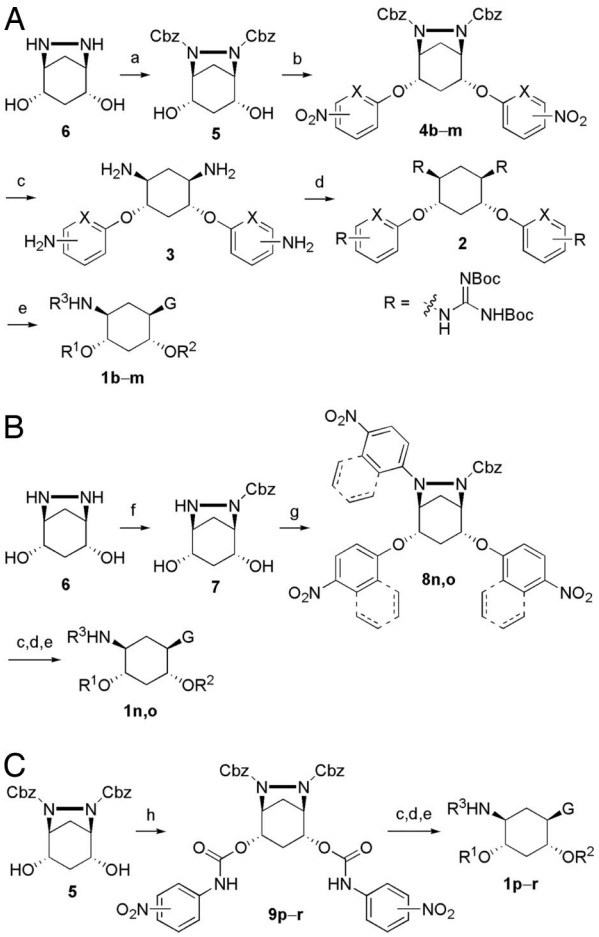

Fig. 2. Syntheses of GADDs. Reagents and conditions were as follows. (*A*) (*a*) 2 eq. of Cbz-Cl, dioxane, H_2O, room temperature; (*b*) NaH (or K_2CO_3), dimethylformamide, room temperature; (**4b**) 1 eq. of 1-fluoro-4-nitrobenzene, then 1 eq. of 2,4-dinitrofluorobenzene; (**4 c** and **d**) 1 eq. of 1-fluoro-4-nitronaphthalene, then 1 eq. of 2,4-dinitrofluorobenzene; (**4e**) 1 eq. of 1-fluoro-4-nitrobenzene, then 1 eq. of 1-fluoro-4-nitronaphthalene; (**4f**) 2 eq. of 1-fluoro-4-nitronaphthalene; (**4g**) 2 eq. of 1-fluoro-4-nitrobenzene; (**4h**) 2 eq. of 1-fluoro-2-nitrobenzene; (**4i**) 2 eq. of 2-chloro-5-nitropyridine; (**4j**) 2 eq. of 2-chloro-3-nitropyridine; (**4k**) 2 eq. of 4-chloro-3-nitropyridine; (**4l**) 2 eq. of 1,2-dinitrofluorobenzene; (**4m**) 2 eq. of 3-chloro-2-nitropyridine; (*c*) H_2, Pd/C, MeOH, room temperature; (*d*) TfON = $C(NHBoc)_2$, pyridine, room temperature; (*e*) TFA, dichloro-methane, room temperature. (*B*) (*f*) 1 eq. of Cbz-NOS, dioxane, H_2O, room temperature; (*g*) NaH, dimethylformamide, room temperature; (**8n**) 3 eq. of 1-fluoro-4-nitrobenzene; (**8o**) 3 eq. of 1-fluoro-4-nitronaphthalene. (*C*) (*h*) pyridine, room temperature; (**9p**) 2 eq. of 4-nitro-phenyl isocynate; (**9q**) 2 eq. of 3-nitro-phenyl isocynate; (**9r**) 2 eq. of 2-nitro-phenyl isocynate.

Discussion

In view of the crucial role of furin in a broad spectrum of human diseases (1–3), it is highly desirable to develop inhibitors of furin for potential therapeutic intervention. In recent years, great success has been achieved on development of protein/peptide-based furin inhibitors (9–24). In addition to their excellent potency against furin, the therapeutic potential of protein/peptide-based furin inhibitors has been demonstrated in cell-based systems and animal models (5–8). However, the large molecular weight of proteins, the low turnover of proteins and peptides, and the potential cytotoxicity of peptides (18, 21) are likely to limit their usefulness in therapeutic applications. Nonprotein, nonpeptide small molecule inhibitors may provide a means to avoid the drawbacks associated with protein/peptide-based inhibitors. To date, there have been only two reports that describe nonprotein, nonpeptide inhibitors (25, 26) showing moderate potency against furin and, before the present study, to our knowledge, no report on synthetic small molecule inhibitors.

We report here the discovery of GADDs as inhibitors of furin. These compounds behave as competitive inhibitors of furin with nanomolar inhibitory activity unprecedented for small molecule furin inhibitors. Although their potency against furin is comparable to that of a number of protein/peptide-based furin inhibitors, these small molecules are three orders of magnitude more potent than the nonprotein, nonpeptide furin inhibitors reported (25, 26). Structure–activity–relationship analysis revealed that, although the guanidinyl group plays a crucial role for the potency, there was no linear correlation between the number of guanidinyl groups and inhibition of furin being observed. This finding is in contrast to the literature report that the inhibitory activity of polyarginine peptides against furin is strictly correlated with the number of positive charges (36). It is clear that the spatial location of guanidinyl groups defined by their positions on the aryl ring and the linkage between the 2,5-dideoxystreptamine core and the aryl groups was of paramount importance to inhibitory activity.

Counterscreening of the GADDs against the off-target enzymes illustrated that the GADDs are relatively specific furin inhibitors. They are highly selective for furin when compared with non-PC enzymes such as trypsin, LF, and MT1-MMP. Although PC family members PACE4, PC6B, and PC7 have a high similarity of substrate recognition to furin, the GADDs show a preference of furin and PC6B relative to PACE4 and PC7. The observed selectivity of the GADDs for furin and PC6B, which is expressed primarily in the gut (37), is therefore similar to the protein-based inhibitor α_1-PDX (13) but much more selective than other furin inhibitors, such as peptidyl chloromethyl ketones, proteinase inhibitor 8, and α_2-macroglobulin mutants, which display very little selectivity between furin and other enzymes (13). Further modification of the 2,5-dideoxystreptamine scaffold may yield inhibitors specific for furin or the other PCs. However, it should be noted that, if the motivation for the development of furin inhibitors is to counter acute bacterial and viral pathogens such as anthrax and to find potential biodefense agents, a high degree of furin specificity among the PCs may not be a critical factor for initial consideration.

Using the recently published crystal structure of mouse furin in complex with the alkylating inhibitor decanoyl-Arg-Val-Lys-Arg-CH_2Cl (33), it was possible for us to conduct molecular modeling studies to determine a possible binding mode of the GADDs with furin. The *in silico* docking experiments suggested that the GADDs are likely to target the active site of furin, because they show similar occupancy of the major active subsites compared with the peptidyl inhibitor. According to this model, it appears that strong electrostatic interaction exists between the positively charged guanidinyl groups of GADDs and the negatively charge residues of furin, thus allowing for potent inhibition of furin by GADDs.

Anthrax PA has been shown to be processed by furin at the cell surface during the infection (29). The observation that the GADDs inhibit furin-dependent PA processing in the cell-based assay demonstrates their therapeutic potential versus this mode of infection. In addition, the control experiments showing no detectable cytotoxicity imply that the GADDs may have a high therapeutic index. In our study, a high concentration of the GADDs (EC_{50} = 4.2–12.9 μM) was used to block the processing. Similarly, it has been also reported that a very high concentration of hexa-D-arginine peptide (>100 μM) (6), peptidyl chloromethyl ketones (≥50 μM) (38), and α_1-PDX (8 μM) (8) was required to block processing of PA, HIV-1 glycoprotein gp160, and cytomegalovirus gB glycoprotein, respectively. The reason that blocking the PA processing requires GADD concentration >1,000-fold above the K_i is unclear. This discrepancy may be caused by the highly charged nature of these compounds.

In summary, we have discovered a class of 2,5-dideoxystreptamine-derived small molecules, some of which show strong

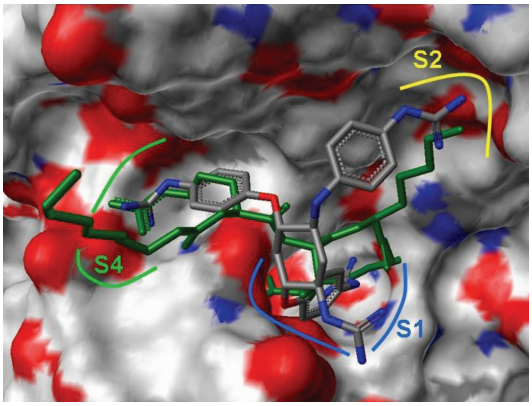

Fig. 3. Docking pose of compound **1n** with the crystal structure position of peptidyl inhibitor decanoyl-Arg-Val-Lys-Arg-chloromethylketone (in green) in the furin active site. The S1 subsite is indicated in blue, the S2 subsite is indicated in yellow, and the S4 subsite is indicated in green.

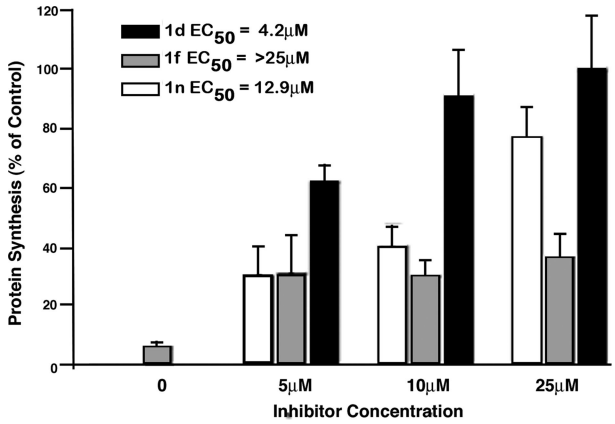

Fig. 4. Cell-based assay efficacy of compounds **1d**, **1f**, and **1n** in the inhibition of furin-dependent processing of PA with LF-*Pseudomonas* exotoxin FP59. RAW 264.7 mouse macrophages were pretreated with the furin inhibitors at the displayed concentrations for 2 h before a 1-h toxin treatment with PA (15 nM) and FP59 (15 nM). Protein synthesis was then quantified by measuring incorporated ^{35}S-Cys/Met after a 1-h pulse label. The value for each bar was normalized to a toxin-free control and represents the average of three assays with error bars showing standard deviation. Linear regression was used to calculate EC_{50} values for each inhibitor. *P* values were: **1d**, 0.0022; **1f**, 0.0172; **1n**, <0.0001.

inhibitory activity against furin in biochemical and cell-based assays. These compounds represent bona fide synthetic small molecule furin inhibitors that exhibit potency in the nanomolar range. We envision that these furin-inhibitory compounds will not only serve as valuable tools for studying how furin functions as an endoprotease, but they may also have therapeutic application as short-term antiviral and antibacterial agents.

Materials and Methods

Materials. All common chemicals, reagents, and buffers were purchased from commercial suppliers and used as received. Pyr-RTKR-MCA was purchased from Peptide Institutes (Osaka, Japan). Anthrax PA and FP59 were kind gifts from Stephen H. Leppla (National Institute of Allergy and Infectious Diseases, Bethesda, MD).

General Procedure for the Synthesis of GADDs. Method A (Fig. 2*A*). ***Step 1.*** To a solution of 6,7-diazobicyclo[3,2,1]octane-(2*S*,4*R*)-2,4-diol **6** (39) (3.000 g, 20.804 mmol) in 90 ml of water/dioxane (1:2, vol/vol), benzyl chloroformate (5.915 ml, 41.608 mmol) was added via a syringe. The reaction mixture was stirred at room temperature for 24 h. The solvent was removed under reduced pressure, and the resulting brown residue was purified by flash column chromatography (230–600 mesh silica gel) eluted with 2% MeOH/CH_2Cl_2 to give compound **5** as a white solid (7.200 g, 84% yield).
Step 2. To a solution of compound **5** (1.000 g, 2.426 mmol) and nitro-substituted aryl halide (4.852 mmol) in 20 ml of dimethylformamide, NaH (60% in mineral oil; 0.107 g, 2.669 mmol) was added quickly. After being stirred at room temperature under N_2 for 48 h, the reaction mixture was diluted with 60 ml of water and extracted with dichloromethane (60 ml × 3). The organic extracts were combined and dried over anhydrous Na_2SO_4. The solvent was removed under reduced pressure, and the resulting brown residue was purified by flash column chromatography (230–600 mesh silica gel) eluting with 0.5% MeOH/CH_2Cl_2 to give the desired compound **4**.
Step 3. To a solution of compound **4** in certain amount of MeOH in a hydrogenation flask, stoimetric Palladium (10 wt % on activated carbon) was added. The flask was put on the Parr apparatus and alternately vacuum-pumped and hydrogen-filled three times. H_2 was then filled to 55 psi. After shaking overnight, the reaction mixture was filtered through a pad of Celite and washed with MeOH. The filtrate was concentrated under reduced pressure, and residue **3** was used directly in the next step without further purification.
Step 4. To a solution of crude compound **3** in 20 ml of pyridine, an excess of *N*,*N*′-di-(*tert*-butoxycarbonyl)-*N*″-triflylguanidine was added. The reaction mixture was stirred at room temperature for 48 h. The solvent was then removed under reduced pressure. The resulting residue was dissolved in 100 ml of dichloromethane and washed with HCl (2 M) and brine. The organic layer was dried over anhydrous Na_2SO_4 and concentrated under reduced pressure. The residue was purified by flash column chromatography (230–600 mesh silica gel) eluted with 1% MeOH/CH_2Cl_2 to give the desired compound **2** as a white solid.
Step 5. To a solution of compound **2** in 3 ml of dichloromethane, trifluoroacetic acid (3 ml) was added. After stirring at room

Table 2. Inhibition constants (K_i) for the 2,5-dideoxystrepatmine-derived small molecules against furin and other enzymes

	K_i, μM					
Enzyme	Compound **1d**	Compound **1e**	Compound **1f**	Compound **1g**	Compound **1i**	Compound **1n**
Furin	0.022 ± 0.002	0.006 ± 0.002	0.069 ± 0.004	0.012 ± 0.003	0.042 ± 0.003	0.046 ± 0.003
PC6B	0.022 ± 0.001	0.004 ± 0.001	0.038 ± 0.001	0.004 ± 0.000	0.015 ± 0.001	0.021 ± 0.001
PACE4	0.213 ± 0.002	0.025 ± 0.002	0.120 ± 0.007	0.041 ± 0.001	0.061 ± 0.004	0.058 ± 0.003
PC7	1.569 ± 0.038	0.415 ± 0.014	0.775 ± 0.043	0.595 ± 0.047	3.192 ± 0.041	1.100 ± 0.076
LF	0.560 ± 0.008	1.002 ± 0.019	5.188 ± 0.008	1.241 ± 0.036	1.716 ± 0.011	3.053 ± 0.015
Trypsin	>200	>200	>200	>200	>200	>200
MT1-MMP	>200	>200	>200	>200	>200	>200

The K_i values are expressed as the mean of three independent experiments ± SEM.

temperature for 3 h, the reaction mixture was concentrated under reduced pressure. The resulting residue was triturated with Et_2O, further washed with Et_2O three times, and dried in vacuum overnight to give the final compound **1** as an off-white solid.

Method B (Fig. 2*B*). ***Step 1.*** Similar to step 1 in method A except that only one equivalent of *N*-(benxoxylcarbonyloxy)-succinimide) was used.

Step 2. Similar to step 2 in method A except that three equivalents of nitro-substituted aryl halide were used.

The other steps are the same as steps 3–5 in method A.

Method C (Fig. 2*C*). ***Step 1.*** Compound 5 (0.500 g, 1.213 mmol) and nitro-phenyl isocynate (2.426 mmol) were dissolved in 10 ml of pyridine. After stirring at room temperature under N_2 for 24 h, the reaction mixture was concentrated under reduced pressure, and the resulting residue was purified by flash column chromatography (230–600 mesh silica gel) eluted with 1% $MeOH/CH_2Cl_2$ to give desired compound **9**.

Other steps. The other steps are the same as steps 3–5 in method A.

Characterization Data for Compounds 1b, 1d—1g, 1i, and 1n. For details see *SI Text*.

Biochemical Cleavage Assay for Furin. Recombinant vaccinia-expressed furin was prepared as described (13). *In vitro* furin inhibition assays were performed in 96-well plates with each 200-μl reaction containing ≈5 nM furin in reaction buffer (100 mM Hepes, pH 7.5/0.5% Triton X-100/1 mM $CaCl_2$). A 10-fold dilution series of the compounds (1 nM to 100 μM) was incubated with furin for 30 min at room temperature before the addition of the fluorescent substrate Pyr-RTKR-MCA (Peptide Institutes) at 100 μM. Reactions were monitored by using a Gemini XS fluorescent microplate reader (SpectraMax; Molecular Devices, Carlsbad, CA) with excitation/emmision wavelengths set at 370/460 nm. Data were collected at 1-min intervals for 15 min. Enzyme velocities (fluorescence units per s) were calculated with Softmax Pro 4. Two independent experiments were performed for each compound. For compounds showing activity < 0.5 μM, the third assay was conducted to generate the K_i values as mean ± SEM. To calculate K_is, the enzyme velocities were plotted vs. Log [I] by using Prism 4 software (GraphPad, San Diego, CA). IC_{50} values were calculated by using nonlinear regression, and K_i was calculated from IC_{50} by using the equation $K_i = IC_{50}/(1 + [\text{Substrate}]/K_m)$ (40).

Counterscreening Enzyme Assays. PACE4, PC6B, PC7, LF, trypsin, and MT1-MMP assays were performed as described in refs. 13, 34, 41, and 42, respectively. PACE4 was kindly provided by M. Tortorella (Pfizer, New York, NY). Recombinant vaccinia virus-expressed PC6B and PC7 were prepared as described (13).

Cell-Based Assay. RAW 264.7 mouse alveolar macrophages (TIB-71; ATCC, Manassas, VA) were cultured in RPMI medium 1610 plus 10% FCS. A total of 1×10^5 cells were seeded per well of 24-well plates 16 h before each assay. Cells were pretreated for 2 h with the synthesized compounds at various concentrations before toxin addition (PA and FP59 both at 15 nM) to the same conditioned media. After 1 h of toxin treatment the media were removed and replaced by DMEM plus ^{35}S (15 μCi per well EXPRE35S35S-protein label; PerkinElmer, Wellesley, MA). After 1 h of labeling, cells were rinsed with PBS and lysed in 250 μl of PBS plus 1% Triton X-100 plus 2 mM EDTA. After vortexing the lysates, 100 μl was transferred to prechilled glass tubes containing 500 μl of PBS plus 0.5% BSA. The mixture was precipitated by the addition of 67 μl of 100% trifluoroacetic acid, and the precipitates were isolated by filtration over Whatman (Middlesex, U.K.) GF/C 24-mm circles using a vacuum manifold. Incorporated label on the filters was quantified with a scintillation counter (Beckman, Fullerton, CA).

***In Silico* Docking Experiments.** Docking studies were conducted by using Tripos FlexX software and Sybyl 7.0; Fig. 4 was generated by using Lithium 2.1. The x-ray crystal structure of mouse furin in complex with a covalent inhibitor was used to prepare the binding site [Protein Data Bank ID code 1P8J (33)].

We thank Drs. S. Leppla and M. Tortorella for reagents, Dr. A. McClelland for helpful discussion, and Ms. L. McKasson and Mr. A. Mehok for analytical assistance. This work was funded by the U.S. Department of Defense, U.S. Army Medical Research and Materials Command, Fort Detrick, MD, and administered by the Pacific Telehealth and Technology Hui, Honolulu, HI, Contract V549P-6073. G.T. is supported by National Institutes of Health Grants DK 37274 and AI 49793.

1. Nakayama K (1997) *Biochem J* 327:625–635.
2. Thomas G (2002) *Nat Rev Mol Cell Biol* 3:753–766.
3. Rockwell NC, Krysan DJ, Komiyama T, Fuller RS (2002) *Chem Rev* 102:4525–4548.
4. Molloy SS, Anderson ED, Jean F, Thomas G (1999) *Trends Cell Biol* 9:28–35.
5. Bassi DE, De Cicco RL, Mahloogi H, Zucker S, Thomas G, Klein-Szanto AJP (2001) *Proc Natl Acad Sci USA* 98:10326–10331.
6. Sarac MS, Peinado JR, Leppla SH, Lindberg I (2004) *Infect Immun* 72:602–605.
7. Sarac MS, Cameron A, Lindberg I (2002) *Infect Immun* 70:7136–7139.
8. Jean F, Thomas L, Molloy SS, Liu G, Jarvis MA, Nelson JA, Thomas G (2000) *Proc Natl Acad Sci USA* 97:2864–2869.
9. Dahlen JR, Jeans F, Thomas G, Foster DC, Kisiel W (1998) *J Biol Chem* 273:1851–1854.
10. Opal SM, Artenstein AW, Cristofaro PA, Jhung JW, Palardy JE, Parejo NA, Lim Y-P (2005) *Infect Immun* 73:5101–5105.
11. Richer MJ, Keays CA, Waterhouse J, Minhas J, Hashimoto C, Jean F (2004) *Proc Natl Acad Sci USA* 101:10560–10565.
12. Oley M, Letzel MC, Ragg H (2004) *FEBS Lett* 577:165–169.
13. Jean F, Stella K, Thomas L, Liu G, Xiang Y, Reason AJ, Thomas G (1998) *Proc Natl Acad Sci USA* 95:7293–7298.
14. Dufour EK, Denault J-B, Bissonnette L, Hopkins PCR, Lavigne P, Leduc R (2001) *J Biol Chem* 276:38971–38979.
15. Lu W, Zhang W, Molloy SS, Thomas G, Ryan K, Chiang Y, Anderson S, Laskowski M, Jr (1993) *J Biol Chem* 268:14583–14585.
16. Van Rompaey L, Ayoubi T, Van de Ven W, Marynen P (1997) *Biochem J* 326:507–514.
17. Komiyama T, Swanson JA, Fuller RS (2005) *Antimicrob Agents Chemother* 49:3875–3882.
18. Liu Z-X, Fei H, Chi C-W (2004) *FEBS Lett* 556:116–120.
19. Komiyama T, VanderLugt B, Fugere M, Day R, Kaufman RJ, Fuller RS (2003) *Proc Natl Acad Sci USA* 100:8205–8210.
20. Cameron A, Appel J, Houghten RA, Lindberg I (2000) *J Biol Chem* 275:36741–36749.
21. Angliker H (1995) *J Med Chem* 38:4014–4018.
22. Villemure M, Fournier A, Gauthier D, Rabah N, Wilkes BC, Lazure C (2003) *Biochemistry* 42:9659–9668.
23. Basak A, Lazure C (2003) *Biochem J* 373:231–239.
24. Basak A, Lotfipour F (2005) *FEBS Lett* 579:4813–4821.
25. Basak A, Cooper S, Roberge AG, Banik UK, Chretien M, Seidah NG (1999) *Biochem J* 338:107–113.
26. Podsiadlo P, Komiyama T, Fuller RS, Blum O (2004) *J Biol Chem* 279:36219–36227.
27. Dixon TC, Meselson M, Guillemin J, Hanna PC (1999) *N Engl J Med* 341:815–826.
28. Petosa C, Collier RJ, Klimpel KR, Leppla SH, Liddington RC (1997) *Nature* 385:833–838.
29. Molloy SS, Bresnahan PA, Leppla SH, Klimpel KR, Thomas G (1992) *J Biol Chem* 267:16396–16402.
30. Klimpel KR, Arora N, Leppla SH (1994) *Mol Microbiol* 13:1093–1100.
31. Leppla SH (1982) *Proc Natl Acad Sci USA* 79:3162–3166.
32. Ascenzi P, Visca P, Ippolito G, Spallarossa A, Bolognesi M, Montecucco C (2002) *FEBS Lett* 531:384–388.
33. Henrich S, Cameron A, Bourenkov GP, Kiefersauer R, Huber R, Lindberg I, Bode W, Than ME (2003) *Nat Struct Biol* 10:520–526.
34. Jiao G-S, Cregar L, Goldman ME, Millis SZ, Tang C (2006) *Bioorg Med Chem Lett* 16:1527–1531.
35. Gordon VM, Rehemtulla A, Leppla SH (1997) *Infect Immun* 65:3370–3375.
36. Kacprzak MM, Peinado JR, Than ME, Appel J, Henrich S, Lipkind G, Houghten RA, Bode W, Lindberg I (2004) *J Biol Chem* 279:36788–36794.
37. Essalmani R, Hamelin J, Marcinkiewicz J, Chamberland A, Mbikay M, Chretien M, Seidah NG (2006) *Mol Cell Biol* 26:354–361.
38. Hallenberger S, Bosch V, Angliker H, Shaw E, Klenk H-D, Garten W (1992) *Nature* 360:358–361.
39. Kavadias G, Velkof S, Belleau B (1978) *Can J Chem* 56:404–409.
40. Cheng Y-C, Prusoff WH (1973) *Biochem Pharmacol* 22:3099–3108.
41. Cregar L, Elrod KC, Putnam D, Moore WR (1999) *Arch Biochem Biophys* 366:125–130.
42. Knight CG, Willenbrock F, Murphy G (1992) *FEBS Lett* 296:263–266.